ChemPubSoc Europe

DOI: 10.1002/cssc.201402928

Synergistic Effect between Defect Sites and Functional Groups on the Hydrolysis of Cellulose over Activated Carbon

Guo Shiou Foo and Carsten Sievers*[a]

The chemical oxidation of activated carbon by H_2O_2 and H_2SO_4 is investigated, structural and chemical modifications are characterized, and the materials are used as catalysts for the hydrolysis of cellulose. Treatment with H_2O_2 enlarges the pore size and imparts functional groups such as phenols, lactones, and carboxylic acids. H_2SO_4 treatment targets the edges of carbon sheets primarily, and this effect is more pronounced with a higher temperature. Adsorption isotherms demonstrate that the adsorption of oligomers on functionalized carbon is dominated by van der Waals forces. The materials treated chemically are active for the hydrolysis of cellulose despite the relative weakness of most of their acid sites. It is proposed that a synergistic effect between defect sites and functional groups enhances the activity by inducing a conformational change in the glucan chains if they are adsorbed at defect sites. This activates the glycosidic bonds for hydrolysis by in-plane functional groups.

Introduction

Cellulose, a linear polysaccharide of glucose monomers linked by β-1,4-glycosidic bonds, is an abundant constituent in most types of biomass.[1] The hydrolysis of cellulose to glucose has been of great interest as the latter is a versatile intermediate for sustainable chemicals and fuels.[2] Mineral acids are inexpensive and display high catalytic activity,[3] but major drawbacks are related to product separation, solvent recycling, and equipment corrosion. Solid acid catalysts offer simplified separation and recycling. Of all the types of solid acid catalysts, carbonaceous solid acids and amorphous carbon seem to be especially effective.[4] Particularly, it has been reported that carbon imparted with sulfonic groups acts as an active, stable, and reusable heterogeneous acid catalyst. Specifically, sulfonated carbon-based acids with a high surface area are preferred.[5]

Many studies focused on the catalytic performance of carbon catalysts, but changes in carbon structure after acid treatment, the role of different functional groups, and mechanistic information remain to be clarified. Besides the use of sulfonated carbon, experiments for the hydrolysis of cellulose have been performed with different solid acids such as niobic acid, Nafion, and Amberlyst-15.[4c,d,6] It was reported that the hydrogen bonds between the phenolic OH groups in carbon and the glycosidic bonds in β-1,4-glucan led to a higher catalytic activity. However, the catalysts were compared with different substrates. Furthermore, the unsulfonated carbon material with carboxylic acid and phenolic groups was not tested for its catalytic activity.

Kobayashi et al. showed that unacidified carbon with oxygen functional groups also displays catalytic activity in the hydrolysis of cellulose.[7] It was further shown that the catalytic activity decreases with the specific amount of functional groups. The hydrolysis of miscanthus xylan was also effective using mesoporous carbon nanoparticles functionalized with weak acid sites.[8] It was argued that strong acid sites such as sulfonic groups could leach through ion exchange in the presence of salts, thus weak acid sites are preferable. However, the mechanism for the hydrolysis of carbohydrates using weak acid sites has not been elucidated fully.

Katz and co-workers grafted β-glucan strands on silica and alumina and found that weakly acidic OH groups with the greatest interactions are able to hydrolyze the glycosidic bond.[9] They also demonstrated that glucan chains can adsorb rapidly onto the surface of mesoporous carbon nanoparticles within the confined pore space.[10] On the basis of these results, it was concluded that the force exerted on the constrained polymer by the pore walls and OH groups leads to the hydrolysis of the glycosidic bond, which relieves some of the mechanical strain.[9c] However, no study has been undertaken to correlate the changes in carbon structure and functional groups as a result of chemical treatment to reactivity.

Here, we report the effects of chemical treatments of activated carbon (AC) with hydrogen peroxide (ACOH) and sulfuric acid at 100 and 200 °C (SAC100 and SAC200) as well as a treatment with hydrogen peroxide followed by sulfuric acid at 100 °C (SACOH). Different types and concentrations of acid sites are imparted by each of these treatments. The effect of the functional groups was determined by adsorption isotherms and the hydrolysis of cellulose. Finally, we examine the origin

[a] G. S. Foo, Prof. C. Sievers
School of Chemical&Biomolecular Engineering
Georgia Institute of Technology
311 Ferst Dr., NW, Atlanta, GA, 30332 (USA)
E-mail: carsten.sievers@chbe.gatech.edu

Supporting Information for this article is available on the WWW under http://dx.doi.org/10.1002/cssc.201402928.

of the catalytic activity, which can be linked to the synergistic effect of functional groups and the immobilization of glucan chains on edge/defect sites.

Results

Characterization

The Raman spectra of all carbon catalysts contained two complex peaks at $\tilde{\nu}=1352$ and 1598 cm^{-1} (Figure 1). These are associated with the vibrational modes of disordered and ordered graphene sheets.[11] However, as a result of the presence of various contributions, the spectra needed to be deconvoluted to obtain the proper structural information (Figure 1). The two peaks were fitted with four Lorentzian-shaped bands (D4, D1, G, and D2) at $\tilde{\nu}=1210$, 1350, 1575, and 1600 cm^{-1}, respectively, and one Gaussian-shaped band (D3) at $\tilde{\nu}=1530$ cm^{-1}.[12] These five components are assigned as polyenes, graphene edges, graphitic carbon, graphene sheets, and amorphous carbon, respectively.

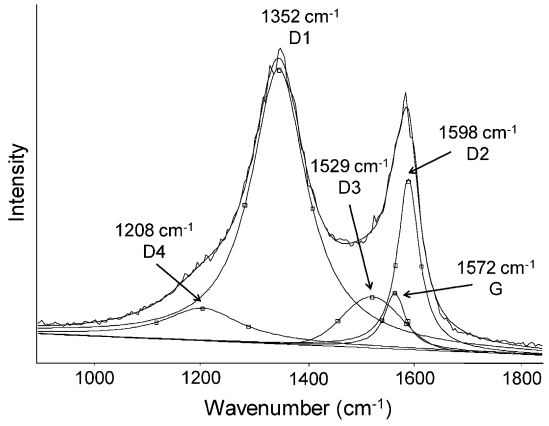

Figure 1. Raman spectrum and results from fitting for AC.

It has been suggested that the ratio $I_{D1}/(I_G+I_{D1}+I_{D2})$ is a measure of the degree of graphitization for carbonaceous materials, in which I is the integral of the fitted peak.[12b,13] The parameter was averaged over three spectra for each sample and is shown in Table 1. The highest values (i.e., the most organized structures) were observed for AC and ACOH, which indicates that the treatment of H_2O_2 did not affect the structural integrity of the sample. Samples treated with H_2SO_4 at 100 °C (SACOH and SAC100) had a lower degree of graphitization, whereas SAC200 had the least organized structure as it was subjected to a more severe treatment. The disorder of the graphene sheets is related to the abundance of edges.[12a] Consequently, it is suggested that H_2SO_4 is able to break down the stacks of graphene sheets and to create step sites at the edge or cavities and that this effect is more pronounced at higher temperatures. The absence of a broad peak at $\tilde{\nu}=500$ cm^{-1} indicates that amorphous sp^3 carbon is not present to a significant extent (Figure S1).[14]

Table 1. Degree of graphitization of carbon catalysts.

Catalyst	$I_{D1}/(I_G+I_{D1}+I_{D2})$
AC	0.745
ACOH	0.746
SACOH	0.733
SAC100	0.729
SAC200	0.715

All of the XRD patterns of the carbon catalysts exhibited two broad peaks at $2\theta=24$ and 42° (Figure S2), which are attributed to the (0 0 2) and (1 0 0) or (1 0 1) planes of graphite crystallites, respectively.[15] This shows that the chemical treatments with H_2O_2 or H_2SO_4 did not change the crystallinity of the carbon structure compared to that of AC to a measurable extent.

The ^{13}C direct-polarization magic-angle spinning (DP MAS) NMR spectra of the carbon samples are shown in Figure S3. The intense and broad peak at $\delta=119$ ppm is assigned to nonprotonated polyaromatic carbon in the core structure.[16] The network of activated carbon is highly complex. As such, the broad peak also contains contributions from exterior carbon species that have a chemical shift that ranges between $\delta=110$ and 148 ppm.[17] As a result of the large range of polyaromatic carbon present, the shoulder caused by carboxylic and phenolic carbon species at $\delta=180$ and 155 ppm can barely be observed. In addition, the low intensity of the resonance of sp^3-hybridized carbon ($\delta=0$–40 ppm) suggests that most of the carbon is polyaromatic and sp^2 hybridized. Deconvolution was attempted, but the resolution of the spectrum was not sufficient to obtain reliable results.

The morphological properties of the carbon catalysts are given in Table 2. Treatments with H_2O_2 and H_2SO_4 had a moder-

Table 2. Surface area, concentration of stable acid sites, and catalytic activity of carbon catalysts.

Catalyst	S_{BET} [$m^2 g^{-1}$]	Concentration of acid site [μmol g^{-1}]				Conversion[c] [%]	Glucose yield [%][c]
		phenolic[a]	lactonic[a]	carboxylic + sulfonic acid[a]	sulfonic acid[b]		
distilled water	–	–	–	–	–	24	0
AC	613	39	58	34	–	27	0
ACOH	634	281	252	244	–	26	2
SACOH	695	233	285	341	31	38	10
SAC100	595	152	115	147	144	32	8
SAC200	653	160	139	163	153	34	10
3.8 mM acetic acid	–	–	–	–	–	23	10
1.8 mM H_2SO_4	–	–	–	–	–	34	18

[a] Determined by Boehm titration. [b] Determined by elemental analysis (S content). [c] Reaction time of 24 h at 150 °C and autogenic pressure.

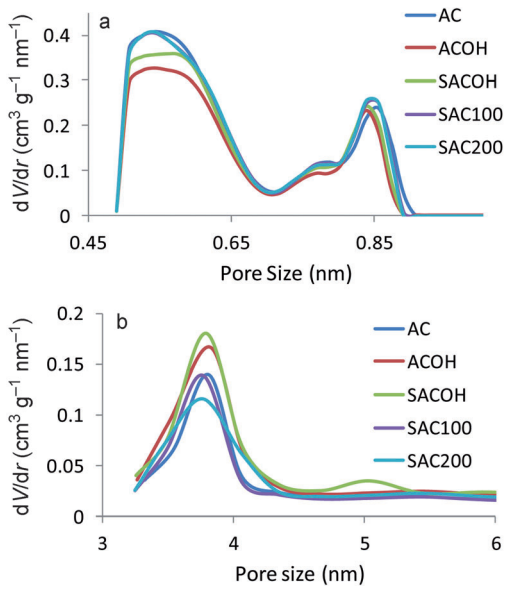

Figure 2. Pore size distribution of carbon catalysts a) 0.45–1.00 nm determined by CO_2 physisorption and b) 3–6 nm determined by N_2 physisorption.

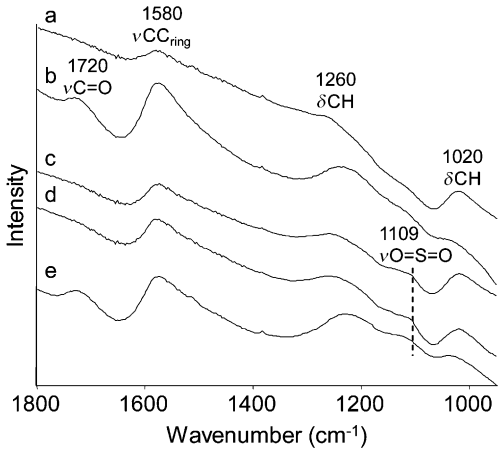

Figure 3. FTIR spectra of a) AC, b) ACOH, c) SAC100, d) SAC200, and e) SACOH.

ate effect on the surface area of the carbon catalysts. The pore volume distribution of the carbon catalysts obtained by both CO_2 and N_2 physisorption is shown in Figure 2. AC oxidized by H_2O_2 showed a decrease in pore volume in the small-pore size range (Figure 2a), whereas there was an increase in pore volume in the larger-pore size range (Figure 2b). Treatment with H_2SO_4 after H_2O_2 (SACOH) led to an increase in pore volume compared to that of ACOH. In addition, there was an increase in pore volume for pore sizes around 5 nm. Acidification by H_2SO_4 at 100 °C (SAC100) did not change the pore volume distribution, whereas acidification at 200 °C (SAC200) decreased the contribution of pores in the larger size range. The pore surface area of the samples showed similar trends (Table S1).

FTIR spectra were measured to identify the types of functional groups present on the carbon samples (Figure 3). All samples displayed a band at $\tilde{\nu} = 1580\ cm^{-1}$ that is assigned to the in-plane vibration of sp^2-hybridized carbon (i.e., C=C).[18] The broad features at $\tilde{\nu} = 1260$ and $1020\ cm^{-1}$ correspond to aromatic δCH.[19] For samples treated with H_2O_2 (Figure 3b and e), a peak at $\tilde{\nu} = 1720\ cm^{-1}$ indicated the presence of carbonyl groups (νC=O). For SAC100 and SAC200 (Figure 3c and d), a broad shoulder was observed at $\tilde{\nu} = 1109\ cm^{-1}$, which is assigned as the $\nu_{sym}SO_3$ for ionic sulfates, whereas the $\nu_{asym}SO_3$ vibration overlapped with the aromatic δCH vibration at approximately $\tilde{\nu} = 1230\ cm^{-1}$.[20] Although this peak was observed for SACOH (Figure 3e), it had a low intensity. These results show that different functional groups were imparted successfully to the carbon structure by different chemical treatments.

For quantitative analysis, only functional groups that were stable for 24 h in liquid water at 150 °C were considered. For ACOH, chemical oxidation by H_2O_2 imparted phenolic, lactonic, and carboxylic acid groups (Table 2). Sequential treatment with H_2O_2 and H_2SO_4 (SACOH) only imparted a small concentration of sulfonic acid groups (31 μmol g^{-1}). However, there was an increase in the concentration of lactonic and carboxylic acid groups and a decrease in phenolic groups. Acidification by H_2SO_4 at 100 °C functionalized the carbon surface mainly with phenolic, lactonic, and sulfonic acid groups. At a higher temperature treatment (SAC200), more of these functional groups are present on the surface. For reference, the concentration of sulfonic acid groups before hot liquid water treatment was also quantified (Table S2).

The pH of the carbon catalysts (300 mg) suspended in 27 mL of deionized (DI) water as well as 3.8 mM acetic acid and 1.8 mM sulfuric acid are given in Table 3. AC displayed the highest pH of 8.4 because of the presence of base sites.[21] The suspension of chemically treated carbon displayed a pH between 4.4 and 5.0, whereas acetic acid and sulfuric acid had a pH of 3.7 and 2.8, respectively.

Table 3. pH values of slurries of 300 mg of each catalyst in 27 mL of water and homogeneous acid solutions used as references.

Catalyst	pH value
AC	8.0
ACOH	5.0
SACOH	4.3
SAC100	4.5
SAC200	4.4
3.8 mM acetic acid	3.7
1.8 mM sulfuric acid	2.8

Hydrolysis of cellulose

Hydrolysis experiments were performed with cellulose that was ball-milled for 48 h to reduce its crystallinity (Figure S4). The resulting material had a slightly lower degree of polymerization (Table S3) and part of it was soluble in water.[22] The AC catalyst gave 27% conversion and 0% glucose yield after 24 h of reaction (Table 2). ACOH provided a similar conversion but had a higher glucose yield of 2%. SACOH showed the highest conversion of 38% and a glucose yield of 10%. SAC100 gave

a glucose yield of 8%, whereas SAC200 had a higher reactivity with a glucose yield of 10%, which is similar to SACOH. The rest of the products were mainly oligomers, which could not be quantified with the analytical setup used here.

For comparison, 27 mL of 3.8 mM acetic acid, which has the same amount of carboxylic acids as SACOH (300 mg), was used in the hydrolysis of cellulose. The glucose yield (10%) was comparable to that of SACOH and SAC200. In addition, 1.8 mM of H_2SO_4 was used for comparison because it has the same concentration of sulfate groups as SAC200. The catalyst exhibited the highest glucose yield of 18%.

The hydrolysis reactions for the carbon catalysts were also performed over various periods of time (Figure 4). SACOH exhibits the highest reactivity followed by SAC200, SAC100, and ACOH. The conversion of cellulose and the glucose yield increased significantly over the first 16 h. For the next 8 h, the glucose yield remained approximately the same, and the increase in conversion was not substantial. These trends are consistent with reports in the literature, which indicated that a plateau is reached for the hydrolysis of cellulose using acidified carbon catalysts.[4a,c,d] This suggests that the remaining cellulose could have a recalcitrant structure that is resistant to hydrolysis by activated carbon.[4a] In addition, reactions with acetic acid and sulfuric acid did not show a net degradation of glucose after 24 h (Figure S5).

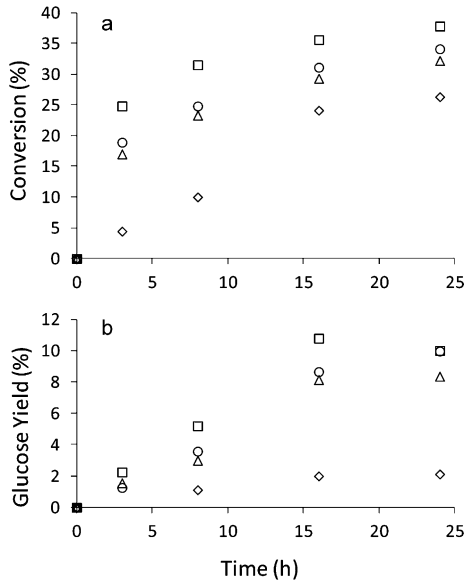

Figure 4. a) Conversion and b) glucose yield during cellulose hydrolysis at 150 °C using chemically treated carbon catalysts: (◇) ACOH, (□) SACOH, (△) SAC100, (○) SAC200.

Adsorption isotherms

To understand how different functional groups on the same carbon substrate influence the adsorption of glucan molecules, adsorption isotherms of glucose and cellobiose were measured. An example of the adsorption isotherms on AC is shown in Figure 5. The maximum uptake values in triplicate experiments were within 10% of each other for the same adsorbent and adsorbate, and all the coefficient of determination (R^2) values were at least 0.95. Adsorption coefficients are within 12–48%. The average maximum uptake (q_m) was normalized by the BET specific surface area of each adsorbent so that comparison between adsorbents can be made. The values of the parameters are summarized in Table 4.

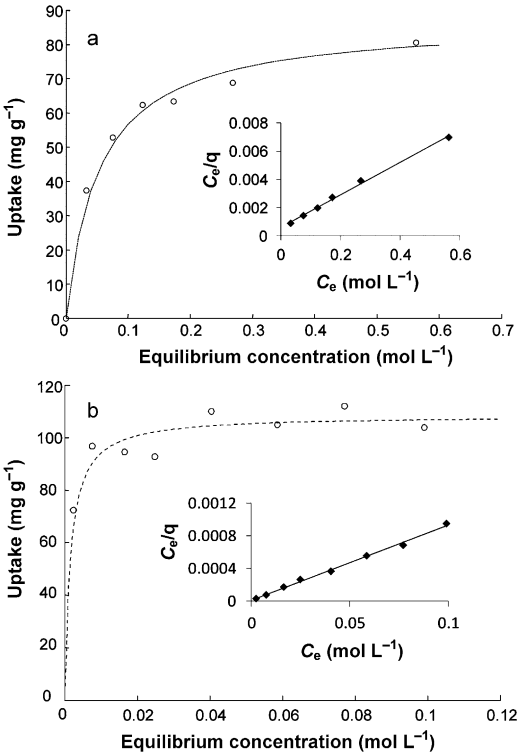

Figure 5. Adsorption isotherms of a) glucose and b) cellobiose on AC. Insets: Linear regression of Langmuir isotherm parameters.

The adsorption coefficient (K) of glucose on AC was 37 L mol^{-1}. If cellobiose was adsorbed on AC, K increased significantly to 650 L mol^{-1}. However, if the bare carbon material was functionalized, K decreased notably. For the adsorption of glucose, K decreased by approximately 60% for the functionalized materials compared to AC. For the adsorption of cello-

Table 4. Langmuir adsorption constant and surface specific maximum uptake for glucose and cellobiose on activated carbon catalysts and change in standard free energy of adsorption between cellobiose and glucose.

Adsorbent	Glucose		Cellobiose		$\Delta\Delta G$
	normalized q_m[a] [mg m^{-2}]	K[b] [L mol^{-1}]	normalized q_m[a] [mg m^{-2}]	K[b] [L mol^{-1}]	[kcal mol^{-1}]
AC	0.135	37	0.171	650	−1.78
ACOH	0.178	13	0.187	379	−1.94
SACOH	0.173	14	0.187	437	−2.03
SAC100	0.192	11	0.200	393	−2.11
SAC200	0.201	16	0.200	402	−2.13

[a] Maximum uptake. [b] Adsorption coefficient.

biose, K also decreased but only by approximately 40%. The change in the standard free energy of adsorption ($\Delta\Delta G$) between the adsorption of cellobiose and glucose was also calculated for each adsorbent (see Supporting Information and Table 4). A negative $\Delta\Delta G$ value of -1.78 kcal mol^{-1} was obtained for AC. For the functionalized carbon materials, the value of $\Delta\Delta G$ decreased to between -1.94 and -2.13 kcal mol^{-1}. The normalized q_m of AC for the adsorption of glucose is 0.135 mg m^{-2}. This increased to around 0.17 mg m^{-2} for ACOH and SACOH, and 0.20 mg m^{-2} for SAC100 and SAC200. However, the normalized q_m for the adsorption of cellobiose did not increase significantly relative to that of AC. The fractional increase was only 9–17%.

Discussion

Effects of chemical oxidation on activated carbon

Chemical oxidation is a common approach to tailor the functionality of activated carbon catalysts.[21] Methods to modify activated carbon include acid, base, microwave, ozone, and plasma treatments.[23] These methods are usually used to enhance the adsorption of organic and inorganic pollutants. It is commonly known that oxidative modifications lead to decreases in surface area and pore volume.[23,24] Most studies in the literature only focus on the quantification of the number of functional groups on carbon catalysts and its correlation to reactivity.[4c–e,25] In contrast, the effect of chemical treatment on the structure of carbon has not been studied extensively.

In the present study, FTIR spectroscopy and Boehm titration results demonstrated that oxidation by H_2O_2 functionalized the surface with phenolic, lactonic, and carboxylic acid groups for ACOH, whereas treatment with H_2SO_4 imparts phenolic, lactonic, and sulfonic acid groups (SAC100). Acidification at a high temperature of 200 °C resulted in the presence of more functional groups. In the case of SACOH, only a small concentration of hydrothermally stable sulfonic groups (31 μmol g^{-1}) was retained on the surface after treatment in liquid water at 150 °C. Prior to the elution step, 150 μmol g^{-1} of sulfonic acid groups was present on the sample (Table S2). In agreement with previous studies, we propose that the treatment with H_2O_2 results in oxidation of sites with unsaturated and dangling bonds terminated with CH or CH_2 groups.[15b,26] It is suggested that this is followed by chemical reactions at the hexatomic–hexatomic boundaries to generate new defects after the initial points of attack are functionalized. This suggests that the second chemical treatment with H_2SO_4 results in sulfonic groups that occupy newly generated sites, which are easier to elude. It is speculated that the functional groups present from the first treatment could create a reactive environment on the carbon surface that are converted to porous domains during the acidification with H_2SO_4, which results in a slightly higher surface area for SACOH.

XRD results showed no noticeable effect of treatments with H_2O_2 and H_2SO_4 on the limited crystallinity of the activated carbon. However, the pore size distribution indicated that oxidation by H_2O_2 decreased the pore volume of the carbon material (ACOH) in the small-pore size range, but the pore volume in the larger-pore size range increased (Figure 2). This suggests that oxidation by H_2O_2 enlarges at least some of the pores of the activated carbon. Generally, two routes are possible: an attack on existing defect sites and electrophilic addition on unsaturated C=C bonds.[27] However, Raman spectroscopy results (Table 1) showed that the degree of graphitization for ACOH remains the same as that of AC. This implies that the ratio of graphene edges to graphitic carbon and graphene sheets is largely the same, which suggests that the material that is removed or redistributed could be amorphous in nature.

In the case of SACOH, acidification with H_2SO_4 after H_2O_2 treatment increased the pore volume for existing pore sizes relative to ACOH (Figure 2), whereas the degree of graphitization decreased (Table 1). SAC100 had a similar pore size distribution to AC, but the degree of graphitization was lower than that of AC, which indicates that acidification with H_2SO_4 at 100 °C creates more edges in the carbon structure. This effect is more pronounced at a high-temperature treatment as indicated by the observation of the lowest degree of graphitization for SAC200. This observation is in agreement with a previous study that showed that intercalated sulfuric acid can exfoliate the structure and attack the active sites of carbons at temperatures higher than 100 °C.[28]

Results from ^{13}C DP MAS NMR spectroscopy showed that a large range of polyaromatic carbon species was present in the materials and that most of the carbon in the structure is sp^2 hybridized. In addition, the absence of a peak between $\tilde{\nu}$ = 400–500 cm^{-1} in the Raman spectra of all the samples (Figure S1) also indicated that amorphous sp^3-hybridized carbon is not present in significant amounts.[14] This suggests that the functional groups that are imparted would have to be positioned around the edges and defect sites of the carbon structure, and in the same plane as the graphene sheet.[18,26,29] Specifically, the functional groups are not positioned perpendicularly to the surface, which limits their accessibility for glucan chains. A simple schematic representation of the structures formed in the chemical oxidation process that can occur at the edge or existing defect sites of a graphene sheet is shown in Figure 6. An aromatic or unsaturated C=C bond can be attacked by a reagent to produce a hydroxyl group.[26] This can be oxidized to form a quinone group or broken up to form a carboxylic acid group in the presence of a strong oxidizing agent. In close proximity, a hydroxyl group and a carboxyl or carbonyl group can condense to form a lactone.[29]

Adsorption properties and locality of functional groups

In studies on the hydrolysis of cellulose using functionalized amorphous carbon, it has been claimed that phenolic groups on carbon form hydrogen bonds with the oxygen atoms in glucan chains, whereas carboxylic and sulfonic acid groups do not function as adsorption sites.[4c,d] However, this conclusion was based on the comparison between different types of catalysts, such as Nafion, niobic acid, and Amberlyst-15, and these materials also differ in other properties.

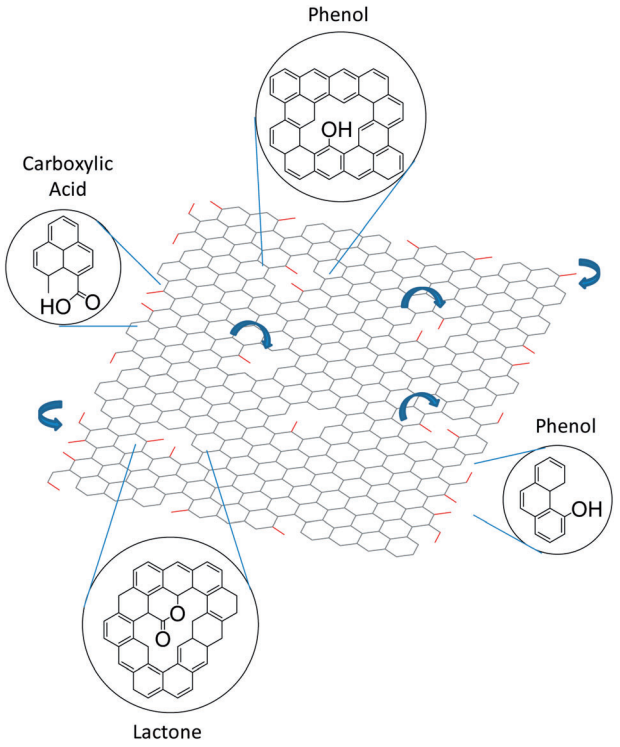

Figure 6. Schematic representation of the structure of functionalized carbon.

In this study, adsorption isotherms revealed that all of the carbon materials are able to adsorb both glucose and cellobiose (Table 4). AC is commonly considered to be a good sorbent for biomass molecules because of its large surface area and pore volume.[30] The adsorption process is driven by van der Waals forces between glucans and the carbon surface.[10] Specifically, it is the interaction between CH groups and the polyaromatic rings.[31] The adsorption of glucose on AC had an adsorption coefficient of 37 L mol^{-1}. However, functionalization of AC reduced the adsorption coefficient of glucose by approximately 60% compared to that of AC. The large decrease is attributed to competitive adsorption with water, which becomes more pronounced as the polarity of the surface increases.

The larger number of CH groups in cellobiose resulted in an increase of the adsorption coefficient on AC to 650 L mol^{-1}. This is attributed to additional van der Waals interactions with the carbon surface. In the case of the functionalized materials, the adsorption coefficients also decreased, but the decrease was less pronounced (40%) compared to the adsorption of glucose. This suggests that the stronger van der Waals interaction allows cellobiose to compete more favorably with water for adsorption sites, even on a relatively polar surface. By extrapolation from the adsorption of glucose and cellobiose, the adsorption coefficients would also increase with the length of the glucan chain, which suggests that the functionalization of the carbon surface has a limited impact on the adsorption of oligomeric species, whereas the adsorption of monomeric glucose is reduced by competition with water. This could explain the limited degradation of glucose monomers in the hydrolysis of cellulose over sulfonated activated carbon.[4a]

The preference for the adsorption of oligomers can be further illustrated by a comparison of the change in the standard free energy of adsorption between cellobiose and glucose ($\Delta\Delta G$). The value for AC was calculated to be -1.78 kcal mol^{-1}, which is close to the value of -1.4 kcal mol^{-1} obtained by Chung et al. for mesoporous carbon nanoparticles.[10] For the functionalized materials, the values of $\Delta\Delta G$ decreased further by up to 0.3 kcal mol^{-1}, which indicates an increase of the preference for the adsorption of cellobiose. As this decrease in the free energy of adsorption is small compared to the strength of a hydrogen bond,[32] it is suggested that interactions with functional groups are not responsible for the difference in adsorption between cellobiose and glucose. Besides solvation, $\Delta\Delta G$ also depends on the degree of contact on the molecular level.[10] We speculate that the defect sites that are formed during the chemical treatment of AC provide a spatial environment that favors the adsorption of cellobiose over glucose.

An increased uptake of glucose monomers was observed on functionalized materials compared to that on AC. One possible explanation is that glucose molecules are adsorbed in an orientation with a smaller footprint on defect sites. Interestingly, SACOH has the same normalized adsorption capacity as ACOH even though it has more functional groups. As the functional groups are located at the edge or defect sites of the graphene sheets (vide supra), this suggests that they are localized in cavities of the carbon structure. Thus, in the case of SACOH, its cavities or edges would have a higher density of functional groups compared to those of ACOH, and there is a limit on the amount of biomass molecules that can be adsorbed in these cavities because of spatial limitations.

A recent report by Fukuoka and co-workers demonstrated that oxygenated functional groups on carbon do not affect the adsorption capacity of glucans, and there was no difference in the adsorption coefficient.[31a] However, the functional groups were removed by heat treatment up to 1273 K, and this method has been shown to also increase the cross-linking of carbon sheets, which could result in a more uniform polyaromatic surface for adsorption.[4b,6] Thus, it is challenging to attribute the observed behavior to a single factor.

Mechanism of cellulose hydrolysis

Reports in the literature have shown that weakly acidic functional groups such as hydroxyl and carboxylic acids on other types of catalysts (niobic acid and Amberlyst) are not active in the hydrolysis of cellulose.[4c,d] However, if they are positioned on a carbon surface, these weak functional groups are able to catalyze the hydrolysis of carbohydrates if the glycosidic bonds are forced to interact with these groups.[7–9] In this study, reactivity results show that only the carbon materials treated chemically yield glucose (Table 2). As no glucose is formed over AC, the weak catalytic activity of ACOH can be ascribed to the addition of the functional groups (i.e., phenolic, lactonic, and carboxylic acid groups). However, the presence of these groups alone provides limited reactivity. The higher catalytic activity of SAC100 and SAC200 could be attributed to the formation of sulfonic acid groups. However, the catalytic activity

of SACOH is comparable to that of SAC200 even though it only has a low concentration of sulfonic groups. In addition, SACOH had only 14.5% more functional groups than ACOH, but its glucose yield was approximately five times higher.

The improvement in catalytic activity for SACOH can be correlated with the degree of graphitization as obtained by Raman spectroscopy (Table 1). Only treatment with H_2SO_4 decreased the degree of graphitization, which decreased more at a higher treatment temperature. The disorder of the carbon structure is attributed to abundant edges.[12a] Thus, we suggest that acidification with H_2SO_4 creates more steps in the cavities or edges of the carbon structure, and these types of defects have a synergistic effect with the in-plane functional groups (vide infra).

Kobayashi et al. ball-milled carbon and cellulose together, and the reactivity of the resulting material was higher than that from an experiment without ball-milling them together.[7] This suggests that intimate interaction between the reactant and catalyst is a prerequisite for hydrolysis. They also showed that salicylic acid, which contains adjacent carboxylic and phenolic groups, is more effective in the hydrolysis of cellobiose than other molecular catalysts such as *m*- and *p*-hydroxybenzoic acid, in which the functional groups are further apart. This illustrates the potential synergistic effects of a coordination site in close proximity to the active site. However, ACOH and SACOH have a similar concentration of weak acid sites, and there is no reason to suggest a preferential formation of paired active sites in SACOH. Furthermore, the pH values of the aqueous slurry of SACOH and SAC200 were 4.3 and 4.4, respectively, which should not be acidic enough to catalyze the hydrolysis reaction. The pH values after reaction were within 0.1 of the original values, which indicates that the functional groups are stable in agreement with a previous report.[21] It was proposed that a pH lower than 4 is needed for this reaction.[33] However, the environment within the vicinity of a sulfonic acid group should still be acidic enough for the reaction to occur. Moreover, the pH values of acetic acid and sulfuric acid used are 3.7 and 2.8, respectively, yet the reactivity of acetic acid did not exceed that of SACOH and SAC200 (Table 2). The slurries of the other carbon catalysts had a higher pH because of the existence of base sites and the delocalization of charge across the basal plane of the carbon surface.[34]

Yanovsky simulated the adsorption of organic polymer chains on different carbon surfaces (with and without defects) and demonstrated that adsorption on a carbon surface with defects is energetically more favorable and that the chains are immobilized in this environment.[35] Furthermore, Gazit and Katz demonstrated that weakly acidic hydroxyl groups on silica and alumina are able to hydrolyze the β-glycosidic bonds by grafting glucan strands on the surface.[9c] This indicates that weakly acidic functional groups are able to perform hydrolysis if they are interacting with a glucan chain in a constraint position. This conclusion is in agreement with a report that concludes that conformational changes in the cellulosic chains are required for the activation of the glycosidic bond for hydrolysis.[36]

On the basis of these findings, it is proposed that the adsorption of glucan chains on defect sites or edges is critical for catalytic activity because a conformational change is induced in this environment. This enables the in-plane functional groups to attack the exposed glycosidic bonds. A schematic representation of the adsorption and hydrolysis process is shown in Figure 7. The analysis of the adsorption isotherms indicates that interactions between the CH groups and polycyclic aromatic rings are responsible for the immobilization of long glucan chains on defect sites. As the functional groups are localized, the probability of hydrolysis increases with the density of functional groups in each defect site. Glucan chains can also adsorb on polyaromatic domains of the carbon surface. However, we speculate that these species are much less susceptible to the hydrolysis reaction because of the lack of functional groups positioned appropriately.

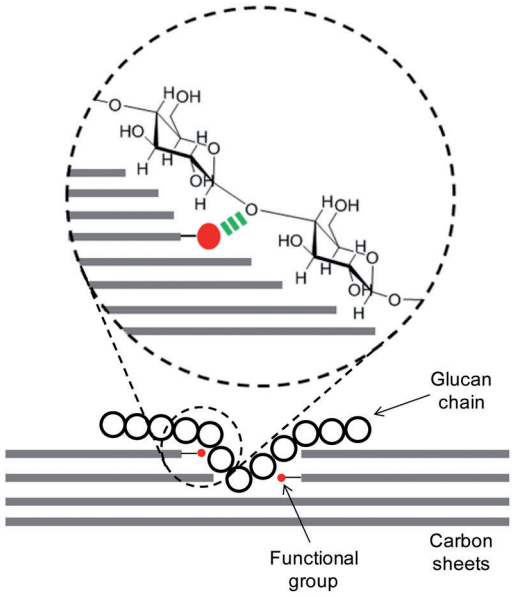

Figure 7. Schematic representation of the adsorption and hydrolysis mechanism.

In a related report, Pang et al. sulfonated carbon at elevated temperatures and reported higher catalytic activity even though the increase in acid density was not significant.[4e] However, beyond a sulfonation temperature of 250 °C, the catalytic activity decreased slightly while the acid site density continued to increase. In the present study, it was found that the degree of graphitization decreases with increasing sulfonation temperature. In addition, the creation of defects and edges in the carbon structure facilitates the hydrolysis of cellulose by a conformation change upon adsorption. We hypothesize that an increase of the sulfonation temperature above 250 °C leads to severe degradation of the carbon structure, which becomes less useful as the defects created could be too large for any effective conformation change of the glucan chain to occur. Chung et al. also reported that there was no proportional cor-

relation between phenolic groups and yield for sulfonated and unsulfonated carbon material in the hydrolysis of miscanthus xylan.[8] This further supports the hypothesis that both functional groups and defect sites are needed for the hydrolysis of glucan chains to occur effectively.

Conclusions

The effect of chemical oxidation on activated carbon was investigated. A simple chemical treatment with H_2O_2 can enlarge pore size and impart hydrophilic functional groups such as phenols, lactones, and carboxylic acids. Treatment with H_2SO_4 decreases the order of graphitization by etching the edges of the carbon structure, and this effect scales with temperature. Only phenols, lactones, and sulfonic groups are functionalized on the carbon material. Extrapolation of the results from adsorption isotherms shows that the functional groups only have a minor effect on the adsorption of long-chain oligomers, which is dominated by van der Waals interactions between CH groups of the sorbate and the surface. The materials treated chemically are more active in the hydrolysis of cellulose compared to homogenous catalysts even though they possess only weakly acidic functional groups. This can be explained by the synergistic effect of functional groups at defect sites and edges of the carbon surface, on which the glycosidic bonds are exposed and forced to interact with the in-plane functional groups.

Experimental Section

Materials

Activated charcoal (untreated, granular, 4–8 mesh, made from peat bog), sulfuric acid (95.0–98.0%), glucose (>99.5%), cellobiose (>98%), sodium hydroxide (>98%, pellets), potassium hydrogen phthalate (>99.95%), sodium carbonate (>99%), sodium bicarbonate (>99.7%), potassium bromide (FTIR grade, >99%), acetic acid (>99.7%), and cellulose (microcrystalline powder) were purchased from Sigma Aldrich. Hydrogen peroxide (30% w/w aqueous solution) and hydrochloric acid (36.5–38.0% w/w aqueous solution) were purchased from BDH and Alfa Aesar, respectively. DI water was further purified by using a Barnstead NANOpure ultrapure water system to 18.2 $M\Omega\,cm^{-1}$.

Synthesis of catalysts

Activated charcoal (2.5 g) was mixed with DI water (30 mL) in a 45 mL Teflon-lined acid digestion vessel (Parr Instrument) and loaded into a rotary oven at 200 °C for 24 h. The material was collected by filtration and washed with DI water. The resulting sample was named AC. Subsequently, AC (0.15 g) was added to H_2O_2 (8.0 g), and the suspension was stirred continuously and heated at 85 °C for 1 h in a beaker. The product was collected by filtration (Fischer Scientific, Grade Q5,5–10 μm), washed with DI water, and named ACOH. To prepare other samples, AC (2.5 g) was mixed with H_2SO_4 (30 mL, 5 M) in a 45 mL Teflon-lined acid digestion vessel (Parr Instrument), loaded into a rotary oven, and heated at 100 and 200 °C for 5 h, respectively. The product was collected by filtration, washed with DI water until the filtrate had a neutral pH, and the samples were named SAC100 and SAC200, respectively. A batch of ACOH was subjected to the same sulfuric acid treatment at 100 °C, and the product was named SACOH. To prevent elution of functional groups during reactions,[21] all chemically treated samples were treated with hot liquid water at 150 °C and autogenic pressure for 24 h, collected by filtration, and washed with DI water until the filtrate had a neutral pH.

Characterization

Raman spectra were collected by using a Confocal Raman Microscope Alpa-Witek with a laser wavelength of 514 nm. Each sample was spread across a glass slide. Ten scans were accumulated and three spectra were obtained for each sample at different locations. Peak fitting was performed with the GRAMS/AI software. XRD measurements were performed by using a Philips X'pert diffractometer equipped with an X'celerator module using CuK_α radiation. Diffractograms were collected at incident angles from $2\theta = 5$ to 70° with a step size of 0.0167°. ^{13}C DP MAS NMR spectroscopic measurements were performed by using a Bruker DSX 300 spectrometer. The samples were packed into a 4 mm zirconia rotor and spun at 10 kHz. Adamantane was used as an external reference material, and the low field peak was set as the reference ($\delta =$ 38.45 ppm). The resonance frequencies of ^1H and ^{13}C were 300.2 and 75.5 MHz, respectively. For ^{13}C detection, high power ^1H decoupling was used during the sampling of the ^{13}C magnetization. A short $\pi/2$ pulse (5 μs) was applied, and the recycle delay was 4 s. Approximately 20000 scans were accumulated for each spectrum. N_2 and CO_2 physisorption measurements were performed by using a Micromeritics ASAP 2020 physisorption analyzer at 77 and 273 K, respectively. Before analysis, approximately 150 mg of each sample was degassed under vacuum for 4 h at 150 °C. For N_2 physisorption, the surface area was calculated using the BET method,[37] and the pore volumes were calculated using the Barrett–Joyner–Halenda (BJH) method.[38] For CO_2 physisorption, the pore volume was calculated using the DFT method.[39] FTIR spectra were collected by using a Nicolet 8700 FTIR spectrometer with a MCT/A detector. For each spectrum, 64 scans were recorded at a resolution of 4 cm^{-1}. Each carbon sample was mixed with KBr at 1 wt%, pressed into a self-supporting wafer, and loaded into a vacuum transmission FTIR chamber. The spectra were taken under vacuum ($<10^{-6}$ mbar). All carbon samples and cellulose were sent to Atlantic Microlab for elemental analysis to determine their sulfur and carbon contents. Boehm titration was performed following procedures reported in the literature to quantify the amount of functional groups present.[21,40] Briefly, each carbon sample (1.5 g) was added to aqueous solutions of NaOH, $NaHCO_3$, and Na_2CO_3 (50 mL), respectively. Each base solution had a concentration of 0.05 M. The slurries were shaken for 24 h, filtered, and 10 mL aliquots of the filtrate were collected. For the $NaHCO_3$ and NaOH solutions, HCl_{aq} (20 mL, 0.05 M) was added. For the Na_2CO_3 solution, HCl_{aq} (30 mL, 0.05 M) was added. The solutions were purged with N_2 for 2 h and back titrated with a 0.05 M solution of NaOH until an endpoint of pH 7.0 was reached. The pH of each carbon catalyst (300 mg) was measured in DI water (27 mL) after 1 h of stirring. During stirring, the suspension was degassed with N_2. The pH of acetic acid (3.8 mM) and sulfuric acid (1.8 mM) was also measured. The weight-average molecular weight (M_w) and number-average molecular weight (M_n) of cellulose and ball-milled cellulose samples were determined by gel permeation chromatography (GPC). This was accomplished by derivatization of the cellulose samples using pyridine and phenyl isocyanate and characterization by using a Waters GPC system. The weight-average and number-average degree of polymerization (DP_w, DP_n) of the cellulose were obtained

by dividing M_w and M_n by 519, the molecular weight of the cellulose tricarbanilate monomer. The molecular weight of the derivatized cellulose samples was determined by using a relative calibration curve. The calibration curve was created by fitting a third polynomial equation to the retention volumes obtained from a series of narrow-molecular-weight-distribution polystyrene standards. The curve fit had an R^2 value of 0.9984.

Hydrolysis of cellulose

As a pretreatment, a batch of cellulose (20 g) was ball-milled in a rotary mill for 48 h at RT. The hydrolysis of ball-milled microcrystalline cellulose was performed in a 100 mL stirred reactor (Parr Instrument). The catalyst (0.300 g), cellulose (0.270 g), and DI water (27 mL) were loaded into the vessel and heated to 150 °C. The mixture was stirred continuously at 500 rpm. After reaction, the aqueous phase was analyzed by HPLC with refractive index detection (RID; Agilent 1260 Infinity HPLC with a Grace Davison Prevail Carbohydrate ES column) to determine the yield of glucose using the same method as for the adsorption isotherms. The conversion of cellulose was determined by mass difference before and after reaction. For this purpose, the samples were dried at RT for 12 h, and it was assumed that the mass of the catalyst remained constant during the reaction.

Adsorption isotherms

Standard glucose solutions were prepared in various concentrations (0.05, 0.1, 0.15, 0.2, 0.3, 0.4, 0.5, and 0.6 M). Standard cellobiose solutions were also prepared in various concentrations (0.01, 0.02, 0.03, 0.04, 0.06, 0.08, 0.10, and 0.12 M). Preweighed amounts of carbon catalysts ($\approx$40 mg) were mixed with sugar solution (1.000 mL) in 1.5 mL microcentrifuge tubes, vortexed for 30 s, and placed on a shaker table for 24 h. The slurries were then centrifuged for 10 min at 10000 rcf. The supernatant was removed and analyzed by HPLC–RID to determine the concentration of the sugar molecules. Accurate concentrations were determined based on an eight-point calibration curve. HPLC–RID analysis was performed by using an Agilent 1260 Infinity HPLC system using a Grace Davison Prevail Carbohydrate ES column. The mobile phase consisted of 75 vol% acetonitrile and 25 vol% water. The flow rate was 1.0 mL min^{-1}, and the injection volume was 0.6 μL. The uptake was calculated by $q=(V(C_0-C_e))/m_{cat}$, in which q is the specific uptake [mol g^{-1}], V is the volume of sugar solution used [L], C_0 and C_e are the initial and equilibrium concentrations of the sugar solution, respectively [mol L^{-1}], and m_{cat} is the mass of carbon material used [g]. Three isotherms were obtained for each molecule on each adsorbent. For each isotherm, the Langmuir isotherm parameters were determined by linear regression (see Supporting Information).

Acknowledgements

The Renewable Bioproducts Institute is acknowledged for the use of its facilities. We thank Johannes Leisen for experimental assistance with ^{13}C DP MAS NMR spectroscopy. Funding from the Georgia Institute of Technology and the U.S. Department of Energy (grant DE-AC36-08-GO28308) is gratefully acknowledged. We thank Matthew Yung for fruitful discussions.

Keywords: acidity · biomass · carbon · hydrolysis · oxidation

[1] G. W. Huber, S. Iborra, A. Corma, *Chem. Rev.* **2006**, *106*, 4044 – 4098.
[2] A. J. Ragauskas, C. K. Williams, B. H. Davison, G. Britovsek, J. Cairney, C. A. Eckert, W. J. Frederick, J. P. Hallett, D. J. Leak, C. L. Liotta, J. R. Mielenz, R. Murphy, R. Templer, T. Tschaplinski, *Science* **2006**, *311*, 484 – 489.
[3] a) E. E. Harris, E. Beglinger, G. J. Hajny, E. C. Sherrard, *Ind. Eng.Chem.* **1945**, *37*, 12 – 23; b) E. E. Harris, E. Beglinger, *Ind. Eng.Chem.* **1946**, *38*, 890 – 895.
[4] a) A. Onda, *J. Jpn. Pet. Inst.* **2012**, *55*, 73 – 86; b) K. Nakajima, M. Hara, *ACS Catal.* **2012**, *2*, 1296 – 1304; c) M. Kitano, D. Yamaguchi, S. Suganuma, K. Nakajima, H. Kato, S. Hayashi, M. Hara, *Langmuir* **2009**, *25*, 5068 – 5075; d) S. Suganuma, K. Nakajima, M. Kitano, D. Yamaguchi, H. Kato, S. Hayashi, M. Hara, *J. Am. Chem. Soc.* **2008**, *130*, 12787 – 12793; e) J. F. Pang, A. Q. Wang, M. Y. Zheng, T. Zhang, *Chem. Commun.* **2010**, *46*, 6935 – 6937.
[5] Y.-B. Huang, Y. Fu, *Green Chem.* **2013**, *15*, 1095 – 1111.
[6] K. Fukuhara, K. Nakajima, M. Kitano, H. Kato, S. Hayashi, M. Hara, *ChemSusChem* **2011**, *4*, 778 – 784.
[7] H. Kobayashi, M. Yabushita, T. Komanoya, K. Hara, I. Fujita, A. Fukuoka, *ACS Catal.* **2013**, *3*, 581 – 587.
[8] P.-W. Chung, A. Charmot, O. A. Olatunji-Ojo, K. A. Durkin, A. Katz, *ACS Catal.* **2014**, *4*, 302 – 310.
[9] a) O. M. Gazit, A. Charmot, A. Katz, *Chem. Commun.* **2011**, *47*, 376 – 378; b) O. M. Gazit, A. Katz, *Langmuir* **2012**, *28*, 431 – 437; c) O. M. Gazit, A. Katz, *J. Am. Chem. Soc.* **2013**, *135*, 4398 – 4402.
[10] P.-W. Chung, A. Charmot, O. M. Gazit, A. Katz, *Langmuir* **2012**, *28*, 15222 – 15232.
[11] A. C. Ferrari, J. Robertson, *Phys. Rev. B* **2000**, *61*, 14095 – 14107.
[12] a) M. Lezanska, P. Pietrzyk, Z. Sojka, *J. Phys. Chem. C* **2010**, *114*, 1208 – 1216; b) A. Sadezky, H. Muckenhuber, H. Grothe, R. Niessner, U. Poschl, *Carbon* **2005**, *43*, 1731 – 1742.
[13] O. Beyssac, B. Goffe, J. P. Petitet, E. Froigneux, M. Moreau, J. N. Rouzaud, *Spectrochim. Acta Part A* **2003**, *59*, 2267 – 2276.
[14] S. Prawer, K. W. Nugent, D. N. Jamieson, J. O. Orwa, L. A. Bursill, J. L. Peng, *Chem. Phys. Lett.* **2000**, *332*, 93 – 97.
[15] a) V. S. Babu, M. S. Seehra, *Carbon* **1996**, *34*, 1259 – 1265; b) A. Manivannan, M. Chirila, N. C. Giles, M. S. Seehra, *Carbon* **1999**, *37*, 1741 – 1747.
[16] H. N. Cheng, L. H. Wartelle, K. T. Klasson, J. C. Edwards, *Carbon* **2010**, *48*, 2455 – 2469.
[17] H. Knicker, K. U. Totsche, G. Almendros, F. J. Gonzalez-Vila, *Org. Geochem.* **2005**, *36*, 1359 – 1377.
[18] C. L. Su, M. Acik, K. Takai, J. Lu, S. J. Hao, Y. Zheng, P. P. Wu, Q. L. Bao, T. Enoki, Y. J. Chabal, K. P. Loh, *Nat. Commun.* **2012**, *3*, 1298.
[19] D. Lennon, D. T. Lundie, S. D. Jackson, G. J. Kelly, S. F. Parker, *Langmuir* **2002**, *18*, 4667 – 4673.
[20] G. Socrates, *Infrared and Raman Characteristic Group Frequencies, 3rd ed.*, Wiley, West Sussex **2001**.
[21] A. H. Van Pelt, O. A. Simakova, S. M. Schimming, J. L. Ewbank, G. S. Foo, E. A. Pidko, E. J. M. Hensen, C. Sievers, *Carbon* **2014**, *77*, 143 – 154.
[22] H. B. Zhao, J. H. Kwak, Y. Wang, J. A. Franz, J. M. White, J. E. Holladay, *Energy Fuels* **2006**, *20*, 807 – 811.
[23] A. Bhatnagar, W. Hogland, M. Marques, M. Sillanpaa, *Chem. Eng. J.* **2013**, *219*, 499 – 511.
[24] a) G. X. Yu, M. Jin, J. Sun, X. L. Zhou, L. F. Chen, J. A. Wang, *Catal. Today* **2013**, *212*, 31 – 37; b) G. G. Stavropoulos, P. Samaras, G. P. Sakellaropoulos, *J. Hazard. Mater.* **2008**, *151*, 414 – 421.
[25] a) X. H. Qi, H. X. Guo, L. Y. Li, R. L. Smith, *ChemSusChem* **2012**, *5*, 2215 – 2220; b) B. B. Chang, J. Fu, Y. L. Tian, X. P. Dong, *J. Phys. Chem. C* **2013**, *117*, 6252 – 6258.
[26] J. Zhang, H. L. Zou, Q. Qing, Y. L. Yang, Q. W. Li, Z. F. Liu, X. Y. Guo, Z. L. Du, *J. Phys. Chem. B* **2003**, *107*, 3712 – 3718.
[27] W. Li, Y. Bai, Y. K. Zhang, M. L. Sun, R. M. Cheng, X. C. Xu, Y. W. Chen, Y. J. Mo, *Synth. Met.* **2005**, *155*, 509 – 515.
[28] Y. Hong, Z. Wang, X. Jin, *Sci. Rep.* **2013**, *3*, 3439.
[29] H. P. Boehm, *Carbon* **1994**, *32*, 759 – 769.
[30] a) J. W. Lee, T. O. Kwon, I. S. Moon, *Carbon* **2004**, *42*, 371 – 380; b) J. W. Yoo, T. Y. Kim, S. Y. Cho, S. G. Rho, S. J. Kim, *J. Ind. Eng. Chem.* **2004**, *10*, 257 – 266.
[31] a) M. Yabushita, H. Kobayashi, J.-y. Hasegawa, K. Hara, A. Fukuoka, *ChemSusChem* **2014**, *7*, 1443 – 1450; b) S. E. Kiehna, Z. R. Laughrey, M. L. Waters, *Chem. Commun.* **2007**, 4026 – 4028; c) Z. R. Laughrey, S. E.

Kiehna, A. J. Riemen, M. L. Waters, *J. Am. Chem. Soc.* **2008**, *130*, 14625 – 14633.
[32] S. Y. Sheu, D. Y. Yang, H. L. Selzle, E. W. Schlag, *Proc. Natl. Acad. Sci. USA* **2003**, *100*, 12683 – 12687.
[33] O. Bobleter, *Prog. Polym. Sci.* **1994**, *19*, 797 – 841.
[34] C. A. Leon y Leon, J. M. Solar, V. Calemma, L. R. Radovic, *Carbon* **1992**, *30*, 797 – 811.
[35] Y. G. Yanovsky, *Nano-Modeling Structure and Micromechanical Properties of Mesoscopic Composite Systems*, Tsinghua University Press, Beijing, **2006**.
[36] C. Loerbroks, R. Rinaldi, W. Thiel, *Chem. Eur. J.* **2013**, *19*, 16282 – 16294.
[37] S. Brunauer, P. H. Emmett, E. Teller, *J. Am. Chem. Soc.* **1938**, *60*, 309 – 319.
[38] E. P. Barrett, L. G. Joyner, P. P. Halenda, *J. Am. Chem. Soc.* **1951**, *73*, 373 – 380.
[39] C. Lastoskie, K. E. Gubbins, N. Quirke, *J. Phys. Chem.* **1993**, *97*, 4786 – 4796.
[40] a) A. M. Oickle, S. L. Goertzen, K. R. Hopper, Y. O. Abdalla, H. A. Andreas, *Carbon* **2010**, *48*, 3313 – 3322; b) S. L. Goertzen, K. D. Theriault, A. M. Oickle, A. C. Tarasuk, H. A. Andreas, *Carbon* **2010**, *48*, 1252 – 1261.

Received: September 1, 2014
Revised: November 10, 2014
Published online on ■■ ■■, 0000

Understanding the hydrolysis of cellulose: Activated carbon is treated chemically with hydrogen peroxide and sulfuric acid to understand the effects of functional groups and morphology on the hydrolysis of cellulose. Defect sites on the carbon surface have been identified as a particularly active environment. Through a synergistic effect with functional groups, glucan chains are hydrolyzed with an increased activity.

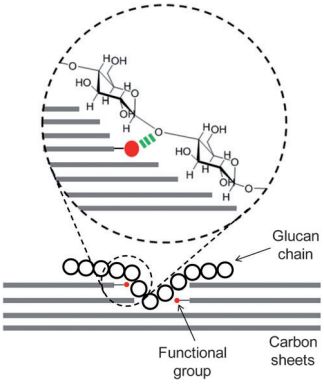

*G. S. Foo, C. Sievers**

■■ – ■■

Synergistic Effect between Defect Sites and Functional Groups on the Hydrolysis of Cellulose over Activated Carbon